Please note this is an author accepted version and NOT the final version:
The final publication is available at Springer via http://dx.doi.org/10.1007/s10522-015-9604-x

Title: Skeletal muscle cells possess a 'memory' of acute early life TNF-α exposure: Role of epigenetic adaptation

Authors: Adam P. Sharples [1] *, Ioanna Polydorou [2,6], David C.Hughes [1,3], Daniel J.Owens [1], Thomas M. Hughes [4,5], Claire E. Stewart [1]

* Corresponding author

Email: a.sharples@ljmu.ac.uk/a.p.sharples@googlemail.com

[1]Stem Cells, Ageing and Molecular Physiology Unit, Exercise Metabolism and Adaptation Research Group, Research Institute for Sport and Exercise Sciences (RISES), School of Sport and Exercise Sciences, Liverpool John Moores University, Liverpool, UK.

[2]Department of Neuropediatrics and NeuroCure Clinical Research Center, Charité—Universitätsmedizin Berlin, Berlin, Germany.

[3]Department of Neurobiology, Physiology and Behavior University of California, Davis, CA, USA.

[4]Sterrenkundig Observatorium Universiteit Gent Krijgslaan Ghent Belgium

[5]Instituto de Física y Astronomía Universidad de Valparaíso Valparaiso Chile

[6]UFR des Sciences de la Santé Université de Versailles Saint-Quentin-en-Yvelines Montigny-Le-Bretonneux, France

Abstract

Sufficient quantity and quality of skeletal muscle is required to maintain lifespan and healthspan into older age. The concept of skeletal muscle programming or memory has been suggested to contribute to accelerated muscle decline in the elderly in association with early life stress such as fetal malnutrition. Further, muscle cells in vitro appear to remember the in vivo environments from which they are derived (e.g. cancer, obesity, type II diabetes, physical inactivity and nutrient restriction). Tumour-necrosis factor alpha (TNF-α) is a pleiotropic cytokine that is chronically elevated in sarcopenia and cancer cachexia. Higher TNF-α levels are strongly correlated with muscle loss, reduced strength and therefore morbidity and earlier mortality. We have extensively shown that TNF-α impairs regenerative capacity in mouse and human muscle derived stem cells (Meadows 2000; Foulstone 2001, 2004; Stewart 2004; Al-Shanti 2008; Saini 2008; Sharples 2010). We have also recently established an epigenetically mediated mechanism (SIRT1-histone deacetylase) regulating survival of myoblasts in the presence of TNF-α (Saini 2012). We therefore wished to extend this work in relation to muscle memory of catabolic stimuli and the potential underlying epigenetic modulation of muscle loss. To enable this aim; C2C12 myoblasts were cultured in the absence or presence of early TNF-α (early proliferative lifespan) followed by 30 population doublings in the absence of TNF-α, prior to the induction of differentiation in low serum media (LSM) in the absence or presence of late TNF-α (late proliferative lifespan). The cells that received an early plus late lifespan dose of TNF-α exhibited reduced morphological (myotube number) and biochemical (creatine kinase activity) differentiation vs. control cells that underwent the same number of proliferative divisions but only a later life encounter with TNF-α. This suggested that muscle cells had a morphological memory of the acute early lifespan TNF-α encounter. Importantly, methylation of myoD CpG islands were increased in the early TNF-α cells, 30 population doublings later, suggesting that even after an acute encounter with TNF-α, the cells have the capability of retaining elevated methylation for at least 30 cellular divisions. Despite these fascinating findings, there were no further increases in myoD methylation or changes in its gene expression when these cells were exposed to a later TNF-α dose suggesting that this was not directly responsible for the decline in differentiation observed. In conclusion, data suggest that elevated myoD methylation is retained throughout muscle cells proliferative lifespan as result of early life TNF-α treatment and has implications for the epigenetic control of muscle loss.

Keywords

Muscle memory; Epigenetics; TNF-alpha; Myoblasts; Muscle stem cell; Proliferative lifespan; Population doublings; Aging; Ageing; myoD; Differentiation; Hypertrophy; Atrophy; Myotube atrophy; Myotube hypertrophy; DNA methylation; CpG methylation; Sarcopenia; Cachexia; Muscle wasting

Introduction

Early evidence for the concept of skeletal muscle 'memory' has emerged from animal studies that investigated a phenomenon defined as 'fetal programming.' This notion referred to alterations in fetal growth and development in response to the prenatal environment having long term or permanent effects in later life. Original works 40 years ago, described early malnutrition during rat pregnancy reducing general cell numbers in the offspring (McLeod et al. 1972). In skeletal muscle it was initially observed that restricted-maternal nutrition by 60 % of the normal energy consumed was found to alter expression of Insulin-like-growth factor II (IGF-II) in ewe foetuses during gestation (Brameld et al. 2000). Since then, a wealth of evidence has suggested that both maternal carbohydrate and amino acid restriction leads to reduced fibre number and size (Fahey et al. 2005; Mallinson et al. 2007), altered protein synthetic signalling (Zhu et al. 2004) and even predisposes the offspring to obesity and type-II diabetes in later life (Samuelsson et al. 2008; Shelley et al. 2009; Zhu et al. 2006). These studies are suggestive of a programming or 'memory' of the foetal environment in the skeletal muscle of the offspring. In humans it has also been demonstrated, through epidemiological studies, that fetal programming and malnutrition have an effect on musculoskeletal development and are associated with changes in body composition into older age (Patel et al., 2010, 2011,2012, 2014, Sayer and Cooper 2005; Sayer et al. 2004). Importantly, reduced weight at birth is correlated with reduced grip strength and decreased muscle size (Funai et al. 2006; Gale et al. 2007; Inskip et al. 2006; Patel et al. 2010, 2011, 2014, 2012; Sayer et al.1998). These factors are associated with increased risk of disability, morbidity and mortality later in life (Gale et al. 2007; Laukkanen et al. 1995; Rantanen 2003; Rantanen et al. 1999, 2002). The molecular mechanisms of such a phenomenon and the concept of skeletal muscle programming/memory, particularly in the regulation of adult skeletal muscle mass growth and loss following changes in anabolic/ catabolic environments throughout the lifespan have not been directly investigated.

Studies into the modulators of skeletal muscle growth alluding to a cellular retention have recently been investigated. Most notably, 3 months of testosterone administration in mice enabled muscle growth accompanied by increased myonuclei number that was retained during subsequent testosterone withdrawal despite muscle loss. The subsequent increase in muscle cross-sectional area following 6 days of mechanical overload was 31 % in the animals that had received an earlier encounter of testosterone vs. controls who demonstrated no significant growth in the same time period (Egner et al. 2013). Further, a similar retention of overload bolstered myonuclei was observed during a subsequent period of denervation induced atrophy (Bruusgaard et al., 2010). While these studies are suggestive of adaptive physical phenomenon and not necessarily cell programming per se, they suggest that muscle retains a cellular potential following prior growth allowing it to respond to future growth stimuli more quickly and perhaps provide protection from periods of muscle loss.

Conversely, skeletal muscle may also remember periods of catabolic environments. At the cellular level our group was the first to demonstrate that where muscle loss occurs in humans with cancer, muscle cells derived from these patients seem to retain a memory of the environment from which they were isolated. These cells exhibited inappropriate proliferative phenotypes in culture versus aged matched healthy controls (Foulstone et al. 2003). Recent studies collectively agree with these findings, confirming muscle derived cells do seem to remember their in vivo environment once isolated from different niches such as type II diabetes (Jiang et al. 2013), obesity (Maples and Brault 2015),

intrauterine growth restriction (Yates et al. 2014) and low physical activity levels (Green et al. 2013; Valencia and Spangenburg 2013).

Although not investigated in the aforementioned studies, the most likely mechanistic underpinning of cellular programming or memory is epigenetic modifications. Epigenetic modifications broadly include histone modifications and DNA methylation that both alter access to enhancer and promoter regions of genes sometimes resulting in altered gene expression. These epigenetic changes have been shown to be transient e.g. methylated for a short period within a cell population following acute environmental stimuli, or extremely stable e.g. being passed to daughter generations of cells, the latter being linked to the concept of cellular programming. Despite its importance, and relevance to muscle adaptability following periods of growth due to hormonal manipulations/overloading exercise or muscle loss in catabolic disease states; research into the epigenetic regulation of gene expression in skeletal muscle is in its infancy. Currently, more data do however exist regarding the epigenetic control of muscle stem cells and the process of myogenesis (Campos et al. 2013; Dilworth and Blais 2011; Hupkes et al. 2011). The muscle specific transcription factor myoD is fundamental in muscle cell lineage determination and for early stages of myoblast differentiation (Blais et al. 2005; Cao et al.2006) via the initiation of p21Cip and irreversible cell cycle exit in G1, a prerequisite for myoblast fusion. MyoD has been shown recently to be bound to a third of gene enhancer regions when a whole genome CHIP assay was performed (Blum et al. 2012), suggesting an important role for myoD in the epigenetic control of muscle cell growth and regeneration. Our group has further begun to elucidate potential epigenetic modulators of myoblast survival and differentiation (Saini et al.2012), where activation of Sirtuin1 (histone deacetylase) reduced myoblast death and enabled differentiation in the presence of stress from TNF-α, a cytokine that is chronically up regulated in muscle loss conditions such as sarcopenia and cachexia. We have extensively shown that TNF-α impairs myoblast fusion/differentiation and myotube hypertrophy with corresponding reductions in myoD gene expression in mouse and human muscle cells (Meadows 2000; Foulstone 2001, 2004; Stewart 2004; Al-Shanti 2008; Saini 2008; Sharples 2010). Thus, together with the above studies, this perhaps provides compelling yet preliminary data suggesting that epigenetic mechanisms such as myoD methylation could be involved in TNF-α induced reduction in differentiation and myotube atrophy in muscle cells and potentially be involved in muscle cell programming/memory.

In an attempt to study the impact of catabolic encounters with TNF-α on the ability of skeletal muscle to remember such an encounter, in the present study we aimed to use a novel cellular model that exposed proliferating myoblasts to an early experimental lifespan stimulus of catabolic TNF-α, followed by multiple population doublings (30 doublings similar to methods used in (Sharples et al. 2011, 2012) in the absence of TNF-α, prior to the induction of differentiation in the absence or presence of a later second experimental lifespan dose of TNF-α. This model allowed us to elucidate whether muscle cells 'remembered' a prior catabolic stress when they encountered it again during differentiation later in their proliferative lifespan and investigate potential epigenetic modulation of muscle cell memory. We hypothesised that an early experimental life encounter with TNF-α would be 'remembered' by skeletal muscle cells when TNF-α was re-encountered in later proliferative life. Also, this memory would be associated with reductions in differentiation and associated myotube atrophy versus relevant control cells that underwent the same number of replicative divisions in vitro without encountering TNF-α. Further, that this increased susceptibility to TNF-α in the presence of a second, later dose of TNF-α would be associated with altered myoD methylation and subsequent changes in myoD gene expression.

Methods

General cell culture

C2C12 mouse skeletal myoblasts (Blau et al. 1985; Yaffe and Saxel 1977) were incubated in T75 flasks in a humidified 5 % CO2atmosphere at 37 °C in growth medium (GM), composed of: DMEM plus 10 % hi fetal bovine serum, 10 % hi newborn calf serum, 1 %l-glutamine (2 mM final), and 1 % penicillin–streptomycin solution, until 80 % confluence was attained. Differentiation experiments were initiated by washing with PBS, and transferring into Low Serum Media (LSM) composed of: DMEM plus 2 % hi horse serum, 1 %l-glutamine, and 1 % penicillin–streptomycin (both as above) in the absence or presence of TNF-α (20 ng ml−1). A dose extensively characterised by ourselves and others to be an inhibitor of differentiation in mouse and human muscle cells (Foulstone et al.2001, 2003, 2004, 2010, 2011; Stewart et al. 2004; Tolosa et al. 2005). C2C12 cells undergo spontaneous differentiation into myotubes on serum withdrawal, and do not require growth factor addition to stimulate the process (Blau et al. 1985; Tollefsen et al.1989).

In-vitro model to assess myoblast programming/memory: Population doubling and establishing the 'early life' encounter with TNF-α

A schematic for deriving the three cell populations (CON, PD, αPD defined below) is depicted in Fig. 1. Briefly, 106 C2C12cells from the same vial were incubated in a pre-gelatinised T75 flask (0.2 % gelatin, Sigma, UK) in GM for 72 h until approximately 80 % confluent. The cells were washed × 2 with PBS and trypsinised, counted and split between three new T75's and left to grow for a 24 h in GM before being washed × 2 with PBS. One flask was transferred to LSM + TNF-α for 48 h and the other two were transferred to LSM alone. There was no sign differentiation/fusion or dead cells (determined by trypan blue exclusion) during this period. One of the LSM alone flasks was trypsinised, centrifuged, pelleted and re-suspended in GM plus 1 % DMSO in cryovials and frozen in liquid nitrogen to create a stock of control (CON) population cells (i.e. no early experimental life dose of TNF-α and no population doublings vs. other daughter populations below). The other LSM alone flask was also trypsinised and plated back onto new T75's in GM where the cells underwent 10 passages (30 population doublings) after which cells were frozen down as described above to derive the population doubled (PD) cell populations. Finally, in parallel to the PD cells the LSM + TNF-α T75 flask was also re-plated and transferred back to GM and passaged ten times (30 divisions) where cells were subsequently frozen down to create the 'early life' TNF-α encounter cell type that had also been population doubled (αPD).

Differentiation experiments

The three cell populations (CON, PD, αPD) were brought up from liquid nitrogen. They were plated at 106 cells.ml−1 in separate T75's in GM and incubated in a humidified 5 % CO2 atmosphere at 37 °C for 72 h until 80 % confluent. Cells were collected following trypsinisation, and were counted in the presence of trypan blue dye. All cells (CON, PD and αPD) were seeded at 8 × 104 cells.ml−1 (in 2 ml) in each well of a six well plate and incubated for 24 h in GM. Cells were washed twice with PBS and transferred to 2 ml LSM.well−1 in the absence or presence of TNF-α (20 ng.ml−1) for up to 72 h (cell treatments and abbreviations can be seen in Table 1). Cells were harvested for counting, total protein and creatine kinase (CK) assays as well as mRNA and DNA for reverse transcription quantitative real time polymerase chain reaction (rt-qRT-PCR) and high resolution melting PCR for gene expression and

DNA (CpG) methlyation respectively. Time point zero (DM0) was defined as 30 min subsequent to transferring into DM ± TNFα. Analytical assays described above and detailed below were performed on at least n = 3/4 independent experiments of the derived cell populations with technical replicates being performed for each independent experiment, details of which can be found in the corresponding figure legends where the data is presented.

Assessment of morphological differentiation

Morphological differentiation was assessed using cell imaging (Leica, DMI 6000 B). All images were obtained at 0 and 72 h following transfer into LSM or TNF-α 20 ng.ml−1. Myotube number, diameter and area were derived from 72 h images using Image J software (Java soft-ware, National Institutes of Health, USA). Myotube number was counted per image and a global mean ± SD across all images per experimental condition was determined (to avoid including cells undergoing mitosis, a myotube was defined as containing 3+ nuclei encapsulated within cellular structures). For myotube diameter (μm); three widths (equidistantly spaced) were calculated on each myotube and averaged to determine the mean width per myotube. Myotube area (μm2) was determined by tracing around myotube structures using image J 'freehand selection' option. To derive mean myotube diameters and areas per treatment, these assessments were repeated for every myotube per image and a global mean ± SD was calculated across all images per cell treatment. Pixel length was converted to μm using Image J and Leica scaling. Morphological analysis was undertaken on images at 20X magnification. Details of number of images analysed per condition can be found in the specific figure legends.

Total protein and creatine kinase activity (biochemical marker of differentiation) assays

Cells were extracted for total protein and CK (creatine kinase) assays at 0 and 72 h. Cells were washed × 2 in PBS, lysed and scraped in 200 μl well−1 0.05 M Tris/MES Triton lysis buffer (TMT: 50 mM Tris-MES, pH 7.8, 1 % Triton X100) and assayed using commercially available BCA™ (Pierce, Rockford, IL, USA) and CK activity (Catachem Inc., Connecticut, N.E, USA) assay kits according to manufacturer's instructions. The enzymatic activity for CK was normalised to total protein content.

RNA isolation, primer design, reverse transcription quantitative real time polymerase chain reaction (rt-qRT-PCR) and analysis

For rt-qRT-PCR experiments cells were lysed in 250 μl/well TRIZOL reagent (Invitrogen Life Technologies, Carlsbad, CA). The RNA was isolated according to manufacturer's instructions and quantified using UV spectroscopy at ODs of 260 and 280 nm, using the Nanodrop spectrophotometer 3000 (Fisher, Rosklide, Denmark). Purity of samples was assessed by 260:280 nm ratio's that ensured end values between 1.9 and 2.15. Identification of primer sequences (see below) was enabled by Gene (NCBI, www.ncbi.nlm.nih.gov/gene) and designed using OligoPerfectTM Designer (Invitrogen, Carlsbad, CA, USA) and/or Primer-BLAST (NCBI, http://www.ncbi.nlm.nih.gov/tools/primer-blast). Primers were purchased from Sigma (Suffolk, UK). Sequence homology (BLAST) searches ensured the primers only matched the intended sequence and therefore gene that they were designed for. Primers were made to exclude self-dimer, hairpins and cross-dimers. All primers designed were between 18 and 23 bp and the GC content ranged between 43 and 50 %. Gene names, Ref. Seq. No., primer sequences and product length were as follows: MyoD, NM_010866.2 Fwd: CATTCCAACCCACAGAAC Rev: GGCGATAGAAGCTCCATA, 125 bp. RPIIb (polr2b), NM_153798.2, Fwd:

GGTCAGAAGGGAACTTGTGGTAT Rev: GCATCATTAAATGGAGTAGCGTC, 197 bp.

rt-qRT-PCR was carried out using QuantiFast™ SYBR® Green RT-PCR one-step kit on a Rotogene 3000Q (Qiagen, Crawley, UK) supported by Rotogene software (Hercules, CA, USA). Reverse transcription was performed on the isolated mRNA at 50 °C (for 10 min), followed by 5 min 95 °C (transcriptase inactivation and initial denaturation), followed by: 10 s, 95 °C (denaturation), 30 s, 60 °C (annealing and extension) for 40 cycles. At the end of the cycling, melt curve analysis (50–99 °C at 1 °C increments) allowed identification of non-specific amplification or primer-dimer issues, none were apparent for the primer sequences listed in above methods. All PCR efficiencies were comparable (93.04 ± 4.32 %) across all conditions and genes. Relative mRNA expression was quantified for myoD using the comparative Ct (ΔΔCt) method (Schmittgen and Livak, 2008) against a stable reference gene of RPIIb (polr2b) (combined Ct value across experimental conditions 16.05 ± 0.31) and calibrator of CON cells in LSM at 0 h.

DNA isolation

Cells were washed × 2 in PBS (2 ml well−1) and incubated for 1.5 h at 37 °C in 250-300 µl of sterile filtered DNA lysis buffer: 1.5 M Tris pH 8.8, (Sigma T1503), 0.25 M EDTA (Sigma E5134), 4 M NaCl, 0.02 % TritonX-100, and 100 µg ml−1 Proteinase K (Sigma P4850). The wells were scraped and cell lysate collected and centrifuged 14,000 rpm at room temperature for 5 min. The supernatant was collected (contains DNA) and an equal volume of isopropanol/NaCl (100 mM) was added and incubated overnight at −20 °C. The sample was next centrifuged for 20 min at 14,000 rpm, the supernatant removed and the DNA pellet reconstituted in TE, pH 8 supplemented with RNase (Ribonuclease A, 10 mg ml−1) and incubated for 1 h at 37 °C before being vortexed and stored for downstream applications at −80 °C. DNA was bisulfite converted (Epitect Bisulfite conversion kits, Qiagen, Manchester, UK) according to manufacturer's instructions and quantified using UV spectroscopy (Nanodrop spectrophotometer 3000, Fisher, Rosklide, Denmark) using the single stranded DNA conversion factor (at 260 nM the coefficient of extinction for single-stranded DNA is 0.027 µg ml−1 cm−1, thus, an OD of 1 corresponds to a concentration of 33 µg ml−1 for single-stranded DNA). Once bisulfite converted, DNA was stored in −80 °C in Qiagen's elution buffer until required for HRM PCR (below).

High resolution melting polymerase chain reaction (HRM PCR) for CpG assays and methylation analysis

20 ng of DNA was used per HRM PCR reaction and carried out using EpiTect™ HRM PCR kits that used Eva Green® as the DNA intercalating fluorescent dye on a Rotogene 3000Q (Qiagen, Crawley, UK) supported by Rotogene software (Hercules, CA, USA). Primer concentrations for CpG assays and EpiTect™ HRM master mix volumes were used according to manufacturer's instructions. CpG assay primers were bought directly from Qiagen. All primers amplified regions containing CpG sites that were located around the myoD promoter associated region i.e. located Chr7:53,632,013-53,632,677. Primers were as follows: (myoD (01) geneglobe cat no; PM00388241, location Chr7: 53,632,013-53,632,218: myoD (02) cat no: PM00388248, location Chr7:53,632,095-53,632,222: myoD (03) cat no: PM00388262, location Chr7:53,632,188-53,632,345: myoD (04) cat no: PM00388269, location Chr7:53,632,463-53,632,677. All primers designed amplified a product between 119 and 214 bp. PCR cycles were as follows: 10 s, 95 °C (denaturation), 30 s, 55 °C (annealing) 10 s, 72 °C extension for a

maximum of 55 cycles. Following PCR a high resolution melt (HRM) protocol was undertaken on the PCR products where the products were melted at 0.1 °C increments from 65 to 95 °C. This gave high resolution melt curves for fluorescence (y axis) versus melt temperature (x axis). A standard curve using the melt analysis was created using methylated mouse DNA standard controls (100, 75, 50, 25, 10, 5, 0 % methylated; EpigenDX, MA, USA) that also underwent the same bisulfite conversion as experimental samples, PCR and HRM as described above (this included a 100 % methylated control sample that had not been bisulfite converted to act as a negative control). All samples were run in duplicate. Duplicate samples were normalised to 0 % methylated controls and averaged to produce a single curve (Fig. 3a). The relationship between the area under the curve, determined from integration of each standard curve, and the corresponding percentage of methylation was defined via the best fitting fourth-order polynomial relation (Fig. 3b). The correlation coefficients we obtained were typically high $r \leq 0.98$ and indicate high precision across the full percentage range. This calibrated relationship was used to quantify the % methylation from the integrated raw melt curves of experimental samples. The percentages were normalised to CON LSM 0 h conditions to indicate fold change in percentage methylation. These calculations were performed using a bespoke Python-based program, MethylCal (T. M. Hughes).

Statistical analyses

Statistical analyses and the significance of the data were determined using minitab version 17.0. Results are presented as mean ± standard deviation (SD). Data were scanned for potential outliers using stem and leaf plots and all data was deemed to be normally distributed and satisfy homogeneity of variance tests. Statistical significance for interactions between cell type (CON, PD, αPD) and dose (DM, TNF-α 20 ng.ml^{-1}) at 72 h was determined using (3 × 2) mixed two-way Factorial ANOVA for all dependent variables (CK, myotube number/diameter/area, myoD transcript expression, and myoD 01,02,03,04 and pooled CpG island methylation. Bonferroni and Tukey post hoc tests were conducted for all pairwise comparisons (unless otherwise stated in the text and as detailed in the figure legends). If Bonferroni pairwise comparisons were not significant and Tukey significant then this was detailed in the figure legends. For all statistical analyses, significance was accepted at $P \leq 0.05$.

Results

Morphological and/ biochemical differentiation and myotube hypertrophy

Basally, 30 population doublings alone (PD) cells demonstrated a significant reduction in differentiation and myotube hypertrophy vs. CON cells (Fig. 2a); where biochemical differentiation/CK activity (PD 345.2 ± 48.4 vs. CON 445.1 ± 60.6 mU.mg.ml−1; $P \leq 0.05$; Fig. 2b), myotube number (PD 2.78 ± 0.833 vs. CON 3.46 ± 0.519; $P \leq 0.05$; Fig. 2c) and myotube area (PD 9335 ± 2468 vs. CON 13,677 ± 2395 μm2; $P \leq 0.05$; Fig. 3e) were significantly reduced, yet myotube diameter unchanged (Fig. 2d). Interestingly, an early experimental life dose of TNF-α followed by 30 population doublings (αPD) was unable to reduce differentiation significantly vs. PD cells alone (myotube number: αPD 2.77 ± 0.439 vs. PD 2.78 ± 0.83; diameter: αPD 21.97 ± 1.67 vs. PD 22.74 ± 2.22 μm, area: αPD 7047 ± 1976 vs. PD 9335 ± 2468 μm2; P = NS; Fig. 2c, d, e respectively) suggesting no impact of an 'early life' encounter with TNF-α after 30 population doublings versus the relevant PD control, at least when cells are induced to differentiate under basal (LSM alone, i.e. no TNF-α) conditions.

TNF-α reduced differentiation (CK and myotube number) and myotube area in CON cells (CK: CON 445.1 ± 60.6 vs. CONα 237.9 ± 47.2 mU.mg.ml−1; myotube number: CON 3.46 ± 0.519 vs. CONα 2.615 ± 0.519; area: CON 13,677 ± 2395 vs. CONα 9577 ± 1924 μm2; all $P \leq 0.05$; Fig. 2b, c, e respectively). Similarly, TNF-α significantly reduced biochemical differentiation in PD cells versus their own basal control (CK: PD 345.2 ± 48.4 vs. PDα 231.5 ± 29.6 mU.mg.ml−1, $P \leq 0.05$; Fig. 2b) where there were also average, yet non-significant reductions in morphological analysis of differentiation and hypertrophy (myotube number: PD 2.78 ± 0.83 vs. PDα 2.0 ± 0.54; diameter: PD 22.74 ± 2.22 vs. PDα 20.3 ± 1.66 μm, P = N.S. Fig. 2c, d). Despite lack of significance on the latter parameters, there were larger absolute reductions in differentiation (myotube number) and hypertrophy (myotube diameter) observed in PD cells with TNF-α administration that resulted in significant differences vs. CON cells in the presence of TNF-α (myotube number: PDα 2.0 ± 0.54 vs. CONα 2.615 ± 0.519; diameter: PDα 20.31 ± 1.66 vs. CONα 22.9 ± 2.35 μm; all $P \leq 0.05$, Fig. 2c, d respectively), with again average but non-significant reductions in myotube area (PDα 7224 ± 2847 vs. CONα 9577 ± 1924 μm2, P = N.S; Fig. 2e).

Importantly, the largest average absolute reductions in differentiation were in cells that had received an early proliferative lifespan encounter with inflammatory cytokine TNF-α and undergone subsequent 30 population doublings and then encountered a later life cytokine challenge during differentiation (αPDα cell population) vs. PD cells without the early encounter with TNF-α, but differentiated in the presence of TNF-α (PDα) (myotube number αPDα 1.54 ± 0.52 vs. PDα 2.0 ± 0.54, diameter αPDα 18.93 ± 1.8 vs. PDα 20.31 ± 1.66, area αPDα 6022 ± 1038 vs. PDα 7224 ± 2847, P = N.S.; Fig. 2c, d, e respectively), where differences in biochemical differentiation (CK activity) resulted in significance (αPDα 165.5 ± 19.81 vs. PDα 231.5 ± 29.6 mU.mg.ml−1, $P \leq 0.05$; Fig. 2b). Overall, the results above lead to significant interactions between dose and cell type for CK activity and myotube area (both $P \leq 0.05$). The cells that had received an early experimental life encounter with TNF-α, retained a memory, at least with respect to differentiation, when they encountered an inflammatory catabolic stress was experienced again during later life differentiation, where these cells showed the lowest average absolute reductions in all parameters versus all other conditions.

MyoD CpG methylation

We next wished to assess the role of CpG island methylation of myoD to evaluate the impact of potential hypo/hypermethylation on corresponding increases or decreases respectively in myoD gene expression (see below). The largest fold increases in methylation above baseline were in cells exposed to the early encounter with TNF-α, expanded over 30 doublings before being cultured in LSM and induced to differentiate versus their relevant controls (PD). This held true across all CpG islands studied (Fig. 3c–g). When analysed further, there was a significant main effect for cell type for all CpG islands investigated (myoD 01: P = 0.05, Fig. 3c; myoD02: P = 0.002, Fig. 3d; myoD03: P = 0.035, Fig. 3e; myoD 04: P = 0.006, Fig. 3f). When relative fold changes were pooled across all CpG assays (Fig. 3g) there was a significant main effect for cell type ($P \leq 0.001$), dose (P = 0.003) and a significant interaction for cell type × dose (P = 0.012). Specifically, there was a significant pairwise comparisons for αPD versus CON and αPDα versus PD for CpG island myoD02 (αPD 1.61 ± 0.07 vs. CON 1.25 ± 0.02, $P \leq 0.05$ and αPDα 1.5 ± 0.07 vs. PD 1.35 ± 0.07, $P \leq 0.05$) and αPD versus PD for CpG island myoD04 (αPD 2.06 ± 0.03 vs. PD 1.36 ± 0.07, $P \leq 0.05$). There were also significant pairwise comparisons (Fisher LSD) between αPD versus PD for CpG island myoD01 (αPD 1.55 ± 0.27 vs. PD 1.3 ± 0.15 and CON 1.23 ± 0.1, $P \leq 0.05$), αPD versus PD and CON for CpG island myoD02 (αPD

1.61 ± 0.07 vs. PD 1.35 ± 0.07 and CON 1.25 ± 0.02, P ≤ 0.05), myoD03 (αPD 2.32 ± 0.21 vs. PD 1.54 ± 0.07 and CON 1.61 ± 0.2, P ≤ 0.05) and myoD04 (αPD 2.06 ± 0.03 vs. PD 1.36 ± 0.07 vs. CON 1.44 ± 0.03, P ≤ 0.05). Importantly, when relative fold change data were pooled across CpG assays (Fig. 3g) there was also a significant pairwise comparisons for αPD vs. PD and CON (αPD 1.89 ± 0.36 vs. PD 1.39 ± 0.12 and vs. CON 1.38 ± 0.12, P ≤ 0.05), suggesting that an acute early experimental life encounter with TNF-α alone is powerful enough to be conserved through 30 population doublings and remain elevated in basal LSM.

Although methylation did not increase further in cells that had experienced an early experimental life encounter with TNF-α and then received a second TNF-α encounter upon differentiation (αPDα), the higher mean levels in αPD were sustained in this condition in myoD01, 02 and 04 (actually reduced for myoD03, yet was not significant) evident by no significant differences with αPD for all CpG islands analysed (all αPDα vs. PDα comparisons, P = N.S.). After pooling all CpG fold changes there was indeed significantly reduced methylation in αPDα conditions vs. αPD (αPDα 1.52 ± 0.13 vs. αPD 1.89 ± 0.36), however, αPDα vs. PDα or PD alone were not significantly different.

MyoD gene expression changes

In the present study TNF-α reduced myoD expression in all cell types resulting in a significant main effect for dose (LSM pooled mean 2.179 vs. TNF-α pooled mean 1.01, P ≤ 0.001; Fig. 4); with significant post hoc comparisons in for LSM control versus TNF-α dosed (CON 2.7 ± 0.57 vs. CON α 1.15 ± 0.55, P ≤ 0.05; PD 1.84 ± 0.34 vs. PDα 0.86 ± 0.47, P ≤ 0.05; αPD 1.91 ± 0.31 vs. αPDα 0.87 ± 0.26, P ≤ 0.05). Furthermore, there was also a significant main effect for cell type (P = 0.028) suggesting that myoD expression was reduced to the greatest extent in the PD and αPD cells versus CON regardless of dose (αPD 1.39, PD 1.35 vs. CON 1.93). Further, TNF-α administration during differentiation resulted in the largest average reductions were in both PD and αPD cell types resulting in a significant difference vs. PD LSM for both cell types (PDα 0.86 ± 0.47 and αPDα 1.032 ± 0.42 vs. PD 1.85 ± 0.34; P ≤ 0.05). Although cells that had undergone an early stimulus with TNF-α, undergone multiple population doublings and received a subsequent dose upon serum withdrawal and differentiation (αPDα cells) exhibited reductions in differentiation, myoD however, was also comparably reduced in PD cells in the presence of TNF-α (PDα 0.86 ± 0.47 and αPDα 1.032 ± 0.42, P = N.S.).

Discussion

The present study demonstrates for the first time that muscle cells exposed to an early experimental life (pre-population doubling) dose of TNF-α (αPD cells) were more susceptible to a subsequent post-population doubling encounter with the same cytokine. The cytokine induced larger absolute reductions in morphological/biochemical differentiation versus relevant non-treated, population doubled control cells. We also present novel findings suggesting that these cells retain increased methylation of myoD following their early experimental 'life' proliferative encounter with TNF-α and retain these hypermethlyated patterns even after a subsequent 30 population doublings. Despite methylation remaining higher with the second later life TNF-α stimulus versus PD alone, it was not further elevated versus cells that received TNF-α at an early proliferative stage alone. This suggested, in opposition to the original hypothesis, that despite an increased susceptibility to reductions in differentiation and associated myotube atrophy in the cells that received an early plus later life dose of TNF-α, myoD methylation does not seem to be driving this morphological response. Furthermore, in disagreement

with the original hypothesis, myoD hypermethylation in these cells did not correspond with reductions in myoD gene expression that appeared to be the same in the cells that had received the early experimental life encounter of TNF-α (αPD cells) versus population doubled (PD) alone cells. Finally, myoD gene expression for both population doubled alone cells (PD) versus those that had received an early experimental life dose of TNF-α and subsequently population doubled (αPD) were not further impaired in the presence of TNF-α during differentiation. Therefore, despite showing that cells that encounter an acute early life insult of TNF-α seem to have increased methylated CpG regions, myoD expression per se may not be the main driver of reduced differentiation observed when these cells encountered a second later life TNF-α insult. We also observed a similar trend to that of myoD for both myogenin and IGF-I gene expression (data not shown) suggesting that MRF's or IGF-I family members were also not the main driver of TNF-α induced reductions in differentiation, which therefore may be hypothesised to come as a result of altered cellular signalling processes e.g. via p38 MAPK phosphorylation as its activity has been previously suggested to be heavily involved in TNF-α induced impairments in differentiation (Chen et al. 2007). However, this requires future investigation as to its role in potential morphological memory observed in the present study. It could also be further hypothesised that after early experimental life doses of inflammatory cytokines, subpopulations of cells may become quiescent once the environmental stress has ceased, harbouring epigenetic alterations that could be preserved over many daughter populations. Therefore, these are the cells that retain altered methylated regions while muscle cell function maybe somewhat preserved in the majority of the population. This is certainly warrants further investigation in the present in vitro model.

Overall, however, we present novel findings that suggest upon administration of a cytokine in early proliferative life, muscle cells increase and retain these hypermethylated regions even after subsequent 30 population doublings. Despite epigenetic mechanisms seemingly not underpinning the worsened biochemical and morphological differentiation following a later life exposure to TNF- α, there never the less appears to be a preservation of epigenetic status in muscle cells following an acute cytokine stress. Future large scale methylome studies to identify CpG islands associating in cis (mapping to gene location) are required in this model to investigate the potential impact of TNF-α on CpG methylation acutely and over time in skeletal muscle cells. These pertinent studies would identify CpG islands across all genes and how/if these regulate the impaired differentiation and myotube hypertrophy experienced in muscle cells that have had early life cytokine encounters.

A so called 'memory' as a concept has been recently alluded to whereby 3 months of testosterone administration in mice enabled muscle growth accompanied by increased myonuclei numbers that, interestingly, were retained during subsequent testosterone withdrawal despite muscle size losses. Most importantly, the subsequent rate of growth response following mechanical overload (resistance exercise) was a 31 % increase in muscle cross-sectional area in the animals that had received an earlier encounter of testosterone (Egner et al. 2013) versus control animals. This accompanied earlier work by the same group that suggested myonuclei acquired by mechanical overload are retained during a subsequent atrophic event (Bruusgaard et al. 2010). While this is an adaptive physical phenomenon and not necessarily cell programming per se, these studies importantly suggest that muscle retains a cellular potential following prior growth allowing it to respond to future growth stimuli more quickly, importantly allowing protection during subsequent periods of muscle loss. In the present study we were investigating differentiation and myotube hypertrophy following a catabolic stress, not the role of prior fused myonuclei following a hypertrophic stimulus. However, the present in vitro model could easily be

manipulated to investigate the impact on established myotubes with a hypertrophic stimulus from testosterone, IGF-I or even exercise stimuli via mechanical stretch or electrical stimulation in vitro in monoloayer or using three dimensional bioengineered skeletal muscle e.g. (Player et al., 2014). It is worth noting that there are limited studies assessing DNA methylation post exercise particularly with respect to a memory of earlier exercise or nutritional encounters. Notably, a recent study in skeletal muscle, demonstrated acute metabolic stress (aerobic exercise) reduces DNA methylation of enhancer regions (hypomethlyation) of genes associated with mitochondrial biogenesis (PGC-1α, PDK4 and PPAR-δ) that presumably in turn allowed increased promoter activity (although not directly investigated) and thus increased corresponding transcript expression (Barres et al. 2012). Similarly a more recent study suggests that acute nutritional manipulation (fasting) in combination with acute exercise also provides evidence of an inverse relationship with DNA methylation and gene expression of important metabolic genes involved in substrate utilization (Lane et al. 2015). However, adaptation in the terms of stable methylation patters after chronic anabolic exercise stimuli or periods of catabolic injury/disuse remains unstudied, as do methylation of genes that control muscle mass.

Our groups' earlier work has shown that human muscle cells derived from negative environment such cancer patients remember the environment from which they were derived where they actually exhibited inappropriate proliferative phenotypes versus aged matched healthy controls (Foulstone et al. 2003). More recently this concept has been confirmed and discussed by four further papers (three original works, one review). They collectively suggest muscle derived cells retain a memory once isolated from different environmental niches: (1) muscle derived cells from humans who are physically active, display an improved ability to uptake glucose and are somewhat protected from palmitate induced insulin resistance versus cells isolated from sedentary humans (Green et al. 2013; Valencia and Spangenburg 2013); (2) muscle derived cells from obese patients do not respond to lipid oversupply with the same gene expression signatures versus control (Maples and Brault 2015); (3) muscle derived cells from intrauterine growth-restricted sheep fetuses exhibit deficiencies in proliferation versus controls (Yates et al. 2014). Importantly all of these studies, highlight that muscle derived stem cells with mitotic potential could be important in the concept of programming/memory in skeletal muscle tissue. The latter is particularly pertinent given a recent in vivo study suggesting protein restriction in maternal rats results in what the authors termed 'metabolic inflexibility' in the resulting offsprings skeletal muscle; where impaired expression of genes that increase the capacity for fat oxidation in response to fasting was observed (Aragao et al. 2014). Given that malnutrition during pregnancy is also associated with the progression of sarcopenia into old age in humans, the mechanisms of muscle memory of negative encounters is a particularly pertinent avenue for future research. The only study, other than the data in this manuscript, to investigate potential epigenetic modulation of cell memory from negative environmental encounters was in a recent study where lipid oversupply in obese patients muscle derived cells possessed increased DNA methylation of PPARδ with subsequent larger reductions in PPARδ gene expression vs. non obese controls (Maples and Brault 2015). Despite the subjects in the control group not being age matched with the obese group, where the obese group were on average almost 7 years older, this study, together with present results, implies that epigenetics could be important in muscle memory and impact on skeletal muscle adaptation and function during negative environmental encounters.

In summary: This study showed that skeletal muscle cells have increased susceptibility in late proliferative life to TNF-α stress when the cells have experienced an earlier, acute TNF-α encounter.

This is suggestive of a morphological memory of catabolic stress in myoblasts. Importantly, muscle cells that have experienced even an acute cytokine stress in early life possess an elevated myoD methylation status that is retained into later proliferative lifespan. Despite this, there were no further increases in myoD methylation or gene expression when these cells experienced a further cytokine stress in later life, suggesting that in this model and at the times points studied, epigenetic control of myoD gene expression was not driving the observed morphological memory of increased susceptibility to TNF-α. It remains to be seen if these observations can be recapitulated in vivo especially when satellite cells are so efficient at proliferating and regenerating muscle, even with age (e.g. Collins et al. 2005, 2007). This study does however suggest an important potential epigenetic mechanism via retention of DNA methylation throughout proliferative lifespan in muscle cells following inflammatory stress that is potentially associated with muscle loss into old age of humans.

References

Al-Shanti N, Saini A, Faulkner SH, Stewart CE. 2008. Beneficial synergistic interactions of TNF-alpha and IL-6 in C2 skeletal myoblasts--potential cross-talk with IGF system. Growth factors (Chur, Switzerland) 26(2):61-73.

Aragao RD, Guzman-Quevedo O, Perez-Garcia G, Manhaes-de-Castro R, Bolanos-Jimenez F (2014) Maternal protein restriction impairs the transcriptional metabolic flexibility of skeletal muscle in adult rat offspring. Br J Nutr 112:1–10

Barres R, Yan J, Egan B, Treebak JT, Rasmussen M, Fritz T, Caidahl K, Krook A, O'Gorman DJ, Zierath JR (2012) Acute exercise remodels promoter methylation in human skeletal muscle. Cell Metab 15(3):405–411

Blais A, Tsikitis M, Acosta-Alvear D, Sharan R, Kluger Y, Dynlacht BD (2005) An initial blueprint for myogenic differentiation. Genes Dev 19(5):553–569

Blau HM, Pavlath GK, Hardeman EC, Chiu CP, Silberstein L, Webster SG, Miller SC, Webster C (1985) Plasticity of the differentiated state. Science 230(4727):758–766

Blum R, Vethantham V, Bowman C, Rudnicki M, Dynlacht BD (2012) Genome-wide identification of enhancers in skeletal muscle: the role of MyoD1. Genes Dev 26(24):2763–2779

Brameld JM, Mostyn A, Dandrea J, Stephenson TJ, Dawson JM, Buttery PJ, Symonds ME (2000) Maternal nutrition alters the expression of insulin-like growth factors in fetal sheep liver and skeletal muscle. J Endocrinol 167(3):429–437

Bruusgaard JC, Johansen IB, Egner IM, Rana ZA, Gundersen K (2010) Myonuclei acquired by overload exercise precede hypertrophy and are not lost on detraining. Proc Natl Acad Sci USA 107(34):15111–15116

Campos C, Valente L, Conceicao L, Engrola S, Fernandes J (2013) Temperature affects methylation of the myogenin putative promoter, its expression and muscle cellularity in Senegalese sole larvae. Epigenetics 8(4):389–397

Cao Y, Kumar RM, Penn BH, Berkes CA, Kooperberg C, Boyer LA, Young RA, Tapscott SJ (2006)

Global and gene-specific analyses show distinct roles for Myod and Myog at a common set of promoters. EMBO J 25(3):502–511

Chen SE, Jin B, Li YP (2007) TNF-alpha regulates myogenesis and muscle regeneration by activating p38 MAPK. Am J Physiol Cell Physiol 292(5):C1660–C1671

Collins CA, Olsen I, Zammit PS, Heslop L, Petrie A, Partridge TA, Morgan JE (2005) Stem cell function, self-renewal, and behavioral heterogeneity of cells from the adult muscle satellite cell niche. Cell 122(2):289–301

Collins CA, Zammit PS, Ruiz AP, Morgan JE, Partridge TA (2007) A population of myogenic stem cells that survives skeletal muscle aging. Stem Cells (Dayton, Ohio) 25(4):885–894

Dilworth FJ, Blais A (2011) Epigenetic regulation of satellite cell activation during muscle regeneration. Stem Cell Res Therapy 2(2):18

Egner IM, Bruusgaard JC, Eftestol E, Gundersen K (2013) A cellular memory mechanism aids overload hypertrophy in muscle long after an episodic exposure to anabolic steroids. J Physiol 591(Pt 24):6221–6230

Fahey AJ, Brameld JM, Parr T, Buttery PJ (2005) The effect of maternal undernutrition before muscle differentiation on the muscle fiber development of the newborn lamb. J Anim Sci 83(11):2564–2571

Foulstone EJ, Meadows KA, Holly JM, Stewart CE (2001) Insulin-like growth factors (IGF-I and IGF-II) inhibit C2 skeletal myoblast differentiation and enhance TNF alpha-induced apoptosis. J Cell Physiol 189(2):207–215

Foulstone EJ, Savage PB, Crown AL, Holly JM, Stewart CE (2003) Adaptations of the IGF system during malignancy: human skeletal muscle versus the systemic environment. Horm Metab Res 35(11–12):667–674

Foulstone EJ, Huser C, Crown AL, Holly JM, Stewart CE (2004) Differential signalling mechanisms predisposing primary human skeletal muscle cells to altered proliferation and differentiation: roles of IGF-I and TNFalpha. Exp Cell Res 294(1):223–235

Funai K, Parkington JD, Carambula S, Fielding RA (2006) Age-associated decrease in contraction-induced activation of downstream targets of Akt/mTor signaling in skeletal muscle. Am J Physiol Regul Integr Comp Physiol 290(4):R1080–R1086

Gale CR, Martyn CN, Cooper C, Sayer AA (2007) Grip strength, body composition, and mortality. Int J Epidemiol 36(1):228–235

Green CJ, Bunprajun T, Pedersen BK, Scheele C (2013) Physical activity is associated with retained muscle metabolism in human myotubes challenged with palmitate. J Physiol 591(Pt 18):4621–4635

Hupkes M, Jonsson MK, Scheenen WJ, van Rotterdam W, Sotoca AM, van Someren EP, van der Heyden MA, van Veen TA, van Ravestein-van Os RI, Bauerschmidt S, Piek E, Ypey DL, van Zoelen EJ, Dechering KJ (2011) Epigenetics: DNA demethylation promotes skeletal myotube maturation. Faseb J

25(11):3861–3872

Inskip HM, Godfrey KM, Robinson SM, Law CM, Barker DJ, Cooper C (2006) Cohort profile: the Southampton Women's Survey. Int J Epidemiol 35(1):42–48

Jiang LQ, Duque-Guimaraes DE, Machado UF, Zierath JR, Krook A (2013) Altered response of skeletal muscle to IL-6 in type 2 diabetic patients. Diabetes 62(2):355–361

Lane SC, Camera DM, Lassiter DG, Areta JL, Bird SR, Yeo WK, Jeacocke NA, Krook A, Zierath JR, Burke LM, Hawley JA (2015) Effects of sleeping with reduced carbohydrate availability on acute training responses. J Appl Physiol (1985):jap.00857.02014

Laukkanen P, Heikkinen E, Kauppinen M (1995) Muscle strength and mobility as predictors of survival in 75–84-year-old people. Age Ageing 24(6):468–473

Mallinson JE, Sculley DV, Craigon J, Plant R, Langley-Evans SC, Brameld JM (2007) Fetal exposure to a maternal low-protein diet during mid-gestation results in muscle-specific effects on fibre type composition in young rats. Br J Nutr 98(2):292–299

Maples JM, Brault JJ (2015) Lipid exposure elicits differential responses in gene expression and DNA methylation in primary human skeletal muscle cells from severely obese women. 47(5):139–146

McLeod KI, Goldrick RB, Whyte HM (1972) The effect of maternal malnutrition on the progeny in the rat. Studies on growth, body composition and organ cellularity in first and second generation progeny. Austral J Exp Biol Med Sci 50(4):435–446

Meadows KA, Holly JM, Stewart CE. 2000. Tumor necrosis factor-alpha-induced apoptosis is associated with suppression of insulin-like growth factor binding protein-5 secretion in differentiating murine skeletal myoblasts. J Cell Physiol 183(3):330-337.

Patel HP, Syddall HE, Martin HJ, Stewart CE, Cooper C, Sayer AA (2010) Hertfordshire sarcopenia study: design and methods. BMC Geriatr 10:43

Patel H, Syddall HE, Martin HJ, Cooper C, Stewart C, Sayer AA (2011) The feasibility and acceptability of muscle biopsy in epidemiological studies: findings from the Hertfordshire Sarcopenia Study (HSS). J Nutr Health Aging 15(1):10–15

Patel HP, Jameson KA, Syddall HE, Martin HJ, Stewart CE, Cooper C, Sayer AA (2012) Developmental influences, muscle morphology, and sarcopenia in community-dwelling older men. J Gerontol A 67(1):82–87

Patel HP, Al-Shanti N, Davies LC, Barton SJ, Grounds MD, Tellam RL, Stewart CE, Cooper C, Sayer AA (2014) Lean mass, muscle strength and gene expression in community dwelling older men: findings from the Hertfordshire Sarcopenia Study (HSS). Calcif Tissue Int 95(4):308–316

Player DJ, Martin NR, Passey SL, Sharples AP, Mudera V, Lewis MP (2014) Acute mechanical overload increases IGF-I and MMP-9 mRNA in 3D tissue-engineered skeletal muscle. Biotechnol Lett 36(5):1113–1124

Rantanen T (2003) Muscle strength, disability and mortality. Scand J Med Sci Sports 13(1):3–8

Rantanen T, Guralnik JM, Foley D, Masaki K, Leveille S, Curb JD, White L (1999) Midlife hand grip strength as a predictor of old age disability. JAMA 281(6):558–560

Rantanen T, Avlund K, Suominen H, Schroll M, Frandin K, Pertti E (2002) Muscle strength as a predictor of onset of ADL dependence in people aged 75 years. Aging Clin Exp Res 14(3 Suppl):10–15

Saini A, Al-Shanti N, Sharples AP, Stewart CE (2012) Sirtuin 1 regulates skeletal myoblast survival and enhances differentiation in the presence of resveratrol. Exp Physiol 97(3):400–418

Samuelsson AM, Matthews PA, Argenton M, Christie MR, McConnell JM, Jansen EH, Piersma AH, Ozanne SE, Twinn DF, Remacle C, Rowlerson A, Poston L, Taylor PD (2008) Diet-induced obesity in female mice leads to offspring hyperphagia, adiposity, hypertension, and insulin resistance: a novel murine model of developmental programming. Hypertension 51(2):383–392

Sayer AA, Cooper C (2005) Fetal programming of body composition and musculoskeletal development. Early Hum Dev 81(9):735–744

Sayer AA, Cooper C, Evans JR, Rauf A, Wormald RP, Osmond C, Barker DJ (1998) Are rates of ageing determined in utero? Age Ageing 27(5):579–583

Sayer AA, Syddall HE, Gilbody HJ, Dennison EM, Cooper C (2004) Does sarcopenia originate in early life? Findings from the Hertfordshire cohort study. J Gerontol 59(9):M930–M934

Schmittgen TD, Livak KJ (2008) Analyzing real-time PCR data by the comparative C(T) method. Nat Protoc 3(6):1101–1108

Sharples AP, Al-Shanti N, Stewart CE (2010) C2 and C2C12 murine skeletal myoblast models of atrophic and hypertrophic potential: relevance to disease and ageing? J Cell Physiol 225(1):240–250

Sharples AP, Al-Shanti N, Lewis MP, Stewart CE (2011) Reduction of myoblast differentiation following multiple population doublings in mouse C(2) C(12) cells: a model to investigate ageing? J Cell Biochem 112(12):3773–3785

Sharples AP, Player DJ, Martin NR, Mudera V, Stewart CE, Lewis MP (2012) Modelling in vivo skeletal muscle ageing in vitro using three dimensional bioengineered constructs. Aging Cell 8(10):1474–9726

Shelley P, Martin-Gronert MS, Rowlerson A, Poston L, Heales SJ, Hargreaves IP, McConnell JM, Ozanne SE, Fernandez-Twinn DS (2009) Altered skeletal muscle insulin signaling and mitochondrial complex II–III linked activity in adult offspring of obese mice. Am J Physiol Regul Integr Comp Physiol 297(3):R675–R681

Stewart CE, Newcomb PV, Holly JM (2004) Multifaceted roles of TNF-alpha in myoblast destruction: a multitude of signal transduction pathways. J Cell Physiol 198(2):237–247

Tollefsen SE, Sadow JL, Rotwein P (1989) Coordinate expression of insulin-like growth factor II and its receptor during muscle differentiation. Proc Natl Acad Sci USA 86(5):1543–1547

Tolosa L, Morla M, Iglesias A, Busquets X, Llado J, Olmos G (2005) IFN-gamma prevents TNF-alpha-induced apoptosis in C2C12 myotubes through down-regulation of TNF-R2 and increased NF-kappaB activity. Cell Signal 17(11):1333–1342

Valencia AP, Spangenburg EE (2013) Remembering those 'lazy' days—imprinting memory in our satellite cells. J Physiol 591(Pt 18):4371

Yaffe D, Saxel O (1977) Serial passaging and differentiation of myogenic cells isolated from dystrophic mouse muscle. Nature 270(5639):725–727

Yates DT, Clarke DS, Macko AR, Anderson MJ, Shelton LA, Nearing M, Allen RE, Rhoads RP, Limesand SW (2014) Myoblasts from intrauterine growth-restricted sheep fetuses exhibit intrinsic deficiencies in proliferation that contribute to smaller semitendinosus myofibres. J Physiol 182:194–201

Zhu MJ, Ford SP, Nathanielsz PW, Du M (2004) Effect of maternal nutrient restriction in sheep on the development of fetal skeletal muscle. Biol Reprod 71(6):1968–1973

Zhu MJ, Ford SP, Means WJ, Hess BW, Nathanielsz PW, Du M (2006) Maternal nutrient restriction affects properties of skeletal muscle in offspring. J Physiol 575(Pt 1):241–250

Table 1. Myoblast differentiation experiments culturing conditions.

Time Point/ Denotation	*Description of Differentiation Culture Conditions*
CON 0	CON cells 30 minutes in LSM
CON 72	CON cells 72 hrs in LSM
CON α 72	CON cells 72 hrs in LSM supplemented with TNF-α (20 $ng.ml^{-1}$)
PD 0	Population doubled cells 30 minutes in LSM
PD 72	Population doubled cells 72 hrs in LSM
PD α 72	Population doubled cells 72 hrs in LSM supplemented with TNF-α (20 $ng.ml^{-1}$)
αPD 0	'Early life' TNF-α (40 $ng.ml^{-1}$) & population doubled cells LSM for 30 minutes
αPD 72	'Early life' TNF-α (40 $ng.ml^{-1}$) & population doubled cells LSM for 72 hrs
αPD α 72	'Early life' TNF-α (40 $ng.ml^{-1}$) & population doubled cells 72 hrs in LSM supplemented with TNF-α (20 $ng.ml^{-1}$)

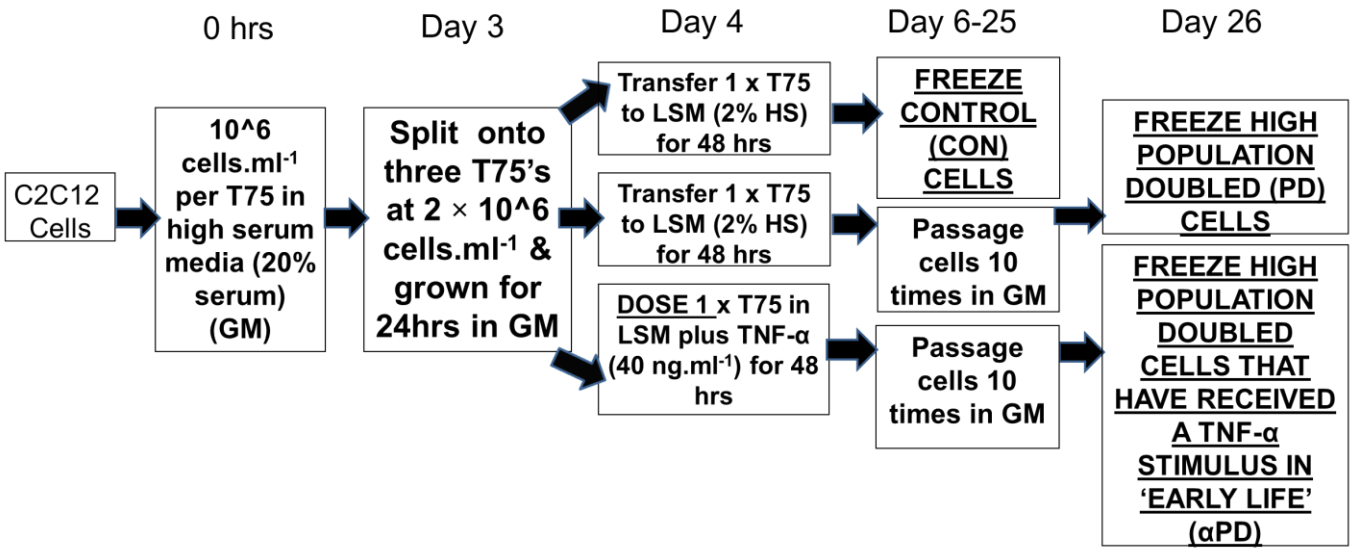

Fig. 1

Schematic diagram for generation of (1) control cells (no doublings relative to population doubled cells, (2) population doubled (PD) cells (30 divisions) and (3) Cell that have had an acute TNF-α exposure in their early proliferative life and subsequently undergo 30 population doublings (αPD).

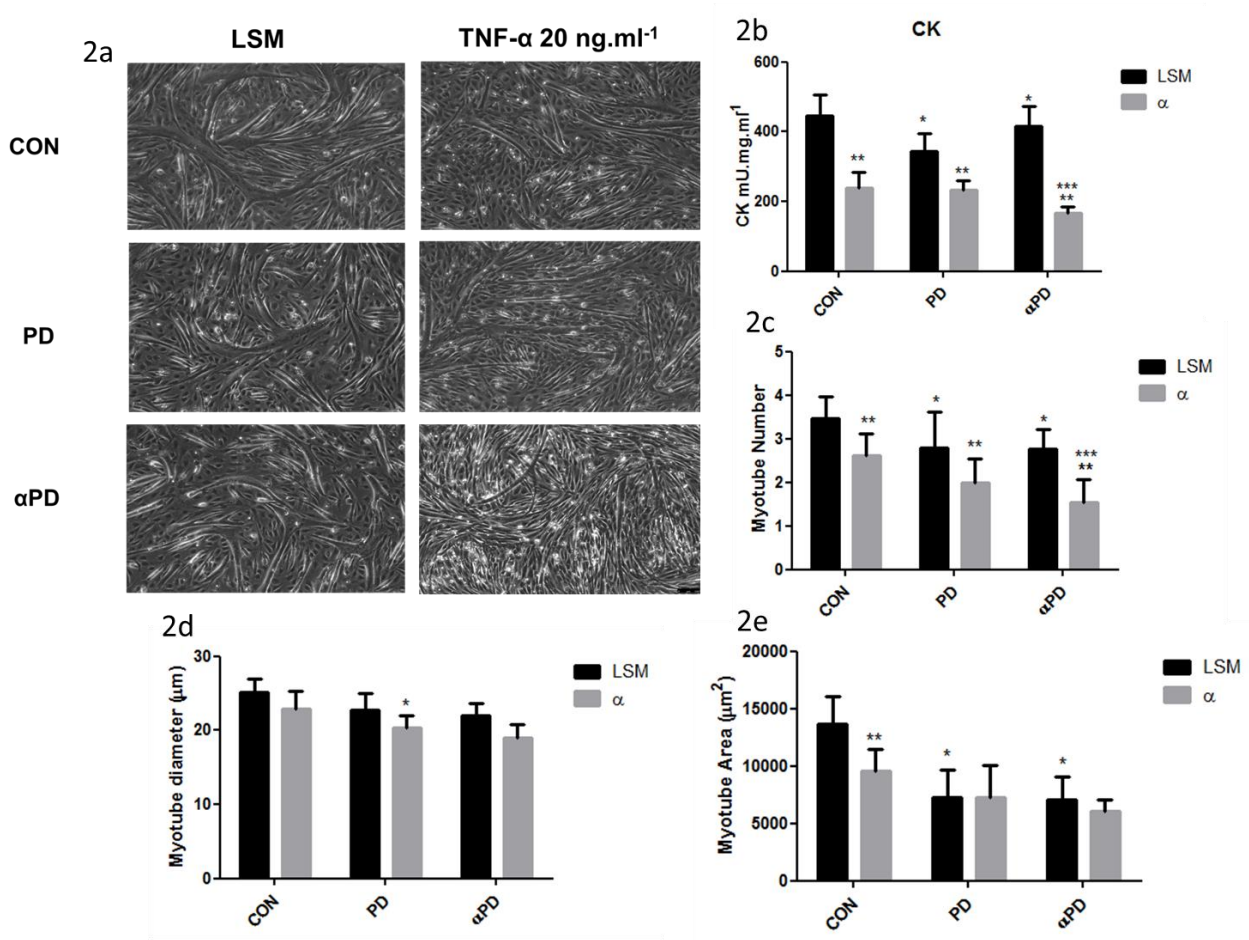

Fig. 2

a. Morphological images (10X) to assess differentiation, myotube number, diameter and area in control (CON), population doubled (PD) and population doubled plus early life acute TNF-α exposure (αPD) cell types at 72 h following transfer into Low serum media (LSM) or LSM plus TNF-α administration (20 ng.ml^{-1}). **b.** Creatine Kinase activity in CON, PD and αPD cells in the absence (LSM) or presence of TNF-alpha (α) CK. *Significantly different to CON LSM 72 h, **significantly different within cell type versus own LSM control, ***significantly different versus PD α. **c.** Myotube number in CON, PD and αPD cells in the absence (LSM) or presence of TNF-alpha (α). *Significantly different to CON LSM, **significantly different within cell type versus own LSM control, ***significantly different vs. CON α. **d.** Myotube diameter in CON, PD and αPD cells in the absence (LSM) or presence of TNF-alpha (α).*Significantly difference versus CON α. **e.** Myotube area in CON, PD and αPD cells in the absence (LSM) or presence of TNF-alpha (α). *Significantly different to CON LSM, **significantly different within cell type versus own LSM control. Morphological analysis was taken from n = 3 or 4 with 4–5 images per n. All significant data were performed using Bonferroni and Tukey post hoc pairwise comparisons.

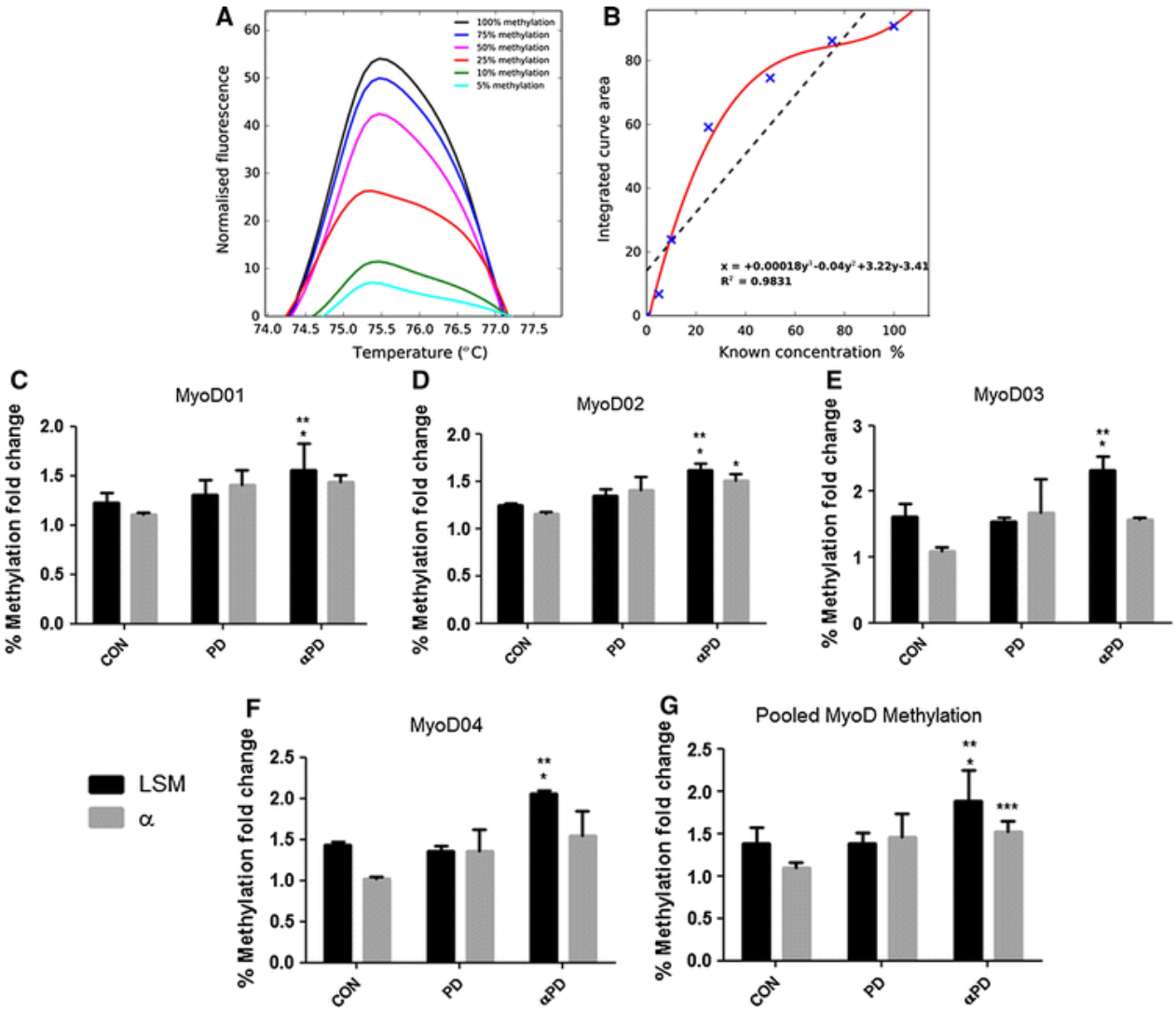

Fig. 3 Relative fold changes of percent myoD CpG island methylation in CON, PD and αPD cells in the absence (LSM) or presence of TNF-alpha (α). a Example of 100, 75, 50, 25, 10, 5, 0 % methylated mouse DNA standard curve with duplicate samples normalised to 0 % methylated controls and averaged to produce a single curve. b An example of the relationship between the area under the curve, determined from integration of each standard curve, and the corresponding percentage of methylation using a best fitting fourth-order polynomial relation. cMyoD01: Location Chr7: 53,632,013-53,632,218. *Significantly different to CON LSM (Fisher LSD pairwise comparison), **significantly different to CON LSM (Fisher LSD pairwise comparison). d MyoD02: location Chr7:53,632,095-53,632,222. *Significantly different to CON LSM (Bonferroni/Tukey pairwise comparisons), **significantly different to PD LSM (Fisher LSD pairwise comparison). e MyoD03: location Chr7:53,632,188-53,632,345. *Significantly different to CON LSM (Fisher LSD pairwise comparison), **significantly different to PD LSM (Fisher LSD pairwise comparison). f MyoD04: location Chr7:53,632,463-53,632,677. *Significantly different to CON LSM (Fisher LSD pairwise comparison), **significantly different to PD LSM (Tukey pairwise comparison only). gPooled myoD CpG island methylation: Location Chr7:53,632,013-53,632,677. *Significantly different to CON LSM (Bonferonni/Tukey pairwise comparisons), **significantly different to PD LSM (Bonferroni/Tukey pairwise comparisons) ***significantly different to αPD (Bonferroni/Tukey pairwise comparisons). Data are representative of n = 3 with the assay ran in duplicate.

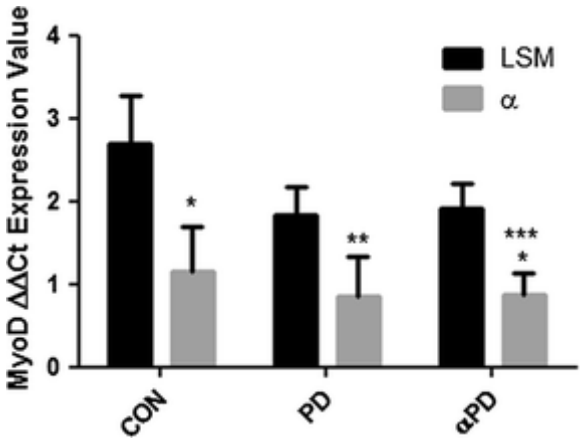

Fig. 4

Relative delta delta Ct expression value for myoD gene transcript expression in CON, PD and αPD cells in the absence (LSM) or presence of TNF-alpha (α). *Significantly different within cell type versus own LSM conditions (Bonferonni and Tukey pairwise comparisons), **significantly different within cell type versus own LSM conditions (Tukey pairwise comparison only), ***significantly different to own PD LSM conditions (Bonferroni and Tukey pairwise comparisons). Data are representative of n = 3 with the assay ran in duplicate.